

RESEARCH ARTICLE

Humidity-mediated changes in an orb spider's glycoprotein adhesive impact prey retention time

Brent D. Opell^{1,*}, Katrina E. Buccella¹, Meaghan K. Godwin², Malik X. Rivas¹ and Mary L. Hendricks¹

ABSTRACT

Properties of the viscous prey capture threads of araneoid orb spiders change in response to their environment. Relative humidity (RH) affects the performance of the thread's hygroscopic droplets by altering the viscoelasticity of each droplet's adhesive glycoprotein core. Studies that have characterized this performance used smooth glass and steel surfaces and uniform forces. In this study, we tested the hypothesis that these changes in performance translate into differences in prey retention times. We first characterized the glycoprotein contact surface areas and maximum extension lengths of *Araneus marmoreus* droplets at 20%, 37%, 55%, 72% and 90% RH and then modeled the relative work required to initiate pull-off of a 4 mm thread span, concluding that this species' droplets and threads performed optimally at 72% RH. Next, we evaluated the ability of three equally spaced capture thread strands to retain a house fly at 37%, 55% and 72% RH. Each fly's struggle was captured in a video and bouts of active escape behavior were summed. House flies were retained 11 s longer at 72% RH than at 37% and 55% RH. This difference is ecologically significant because the short time after an insect strikes a web and before a spider begins wrapping it is an insect's only opportunity to escape from the web. Moreover, these results validate the mechanism by which natural selection can tune the performance of an orb spider's capture threads to the humidity of its habitat.

KEY WORDS: Adhesion, *Araneus marmoreus*, Biomaterial, Extended phenotypic plasticity, Orb web, Viscous capture thread

INTRODUCTION

An orb spider's web is a behavioral and material extension of the spider's phenotype on which the spider relies for prey capture. The web integrates non-adhesive radial and frame threads that absorb and dissipate the kinetic energy of an insect's impact (Sensenig et al., 2012) with spirally arrayed, adhesive prey capture threads (Sahni et al., 2013) that retain the insect until the spider can locate, run to, and begin to subdue it (Chacón and Eberhard, 1980). Thus, material invested in non-adhesive threads increases the size and velocity of insects that a web can successfully stop and material invested in capture thread increases the time a spider has to prevent an insect from escaping. A retention time difference of even 5 s often means the difference between a prey captured or a prey lost (Blackledge and Zevenbergen, 2006; Eberhard, 1989).

Both the non-adhesive and adhesive components of orb webs exhibit phenotypic plasticity (Blamires, 2010; Boutry and Blamires, 2013; Dawkins, 1982). Differences in diet and prey type cause striking differences in both a web's architecture and the properties of its threads (Blamires et al., 2016; Herberstein and Tso, 2011; Scharf et al., 2011; Townley et al., 2006; Tso et al., 2007), as can environmental factors such as wind (Wu et al., 2013). After a web has been spun, its frame and axial threads and its capture threads respond to daily changes in environmental conditions, with humidity having the greatest impact (Agnarsson et al., 2009; Sahni et al., 2011; Opell et al., 2011, 2013; Stellwagen et al., 2014, 2015; Amarpuri et al., 2015).

As explained more fully in the following paragraphs, studies of the effect of humidity on the adhesion of capture threads have concluded that they evolved to perform optimally in the humidity regime typical of a species' habitat (Opell et al., 2013; Amarpuri et al., 2015). In characterizing this performance, these studies have used flat glass and steel contact surfaces and constant velocity extensions to ensure uniform and precise comparisons. However, in nature, capture threads must resist forces whose direction and magnitude change randomly and rapidly and must adhere to three-dimensional, non-uniform insect surfaces, across which adhesion differs greatly (Opell and Schwend, 2007). Because successful prey capture appears to be the only mechanism by which natural selection tunes the humidity-specific performance of an orb web, it is important to verify the link between a thread's fine-scale material properties and its ability to retain prey. The objective of the current study was to document this association.

Modern (Araneoidea) orb spiders employ viscous capture threads, which are formed of regularly spaced droplets (Fig. 1A), each composed of an adhesive glycoprotein core surrounded by a hygroscopic aqueous layer (Fig. 1B; Edmonds and Vollrath, 1992; Townley et al., 1991; Sahni et al., 2013; Townley and Tillinghast, 2013; Opell et al., 2015). These threads are spun as a continuous cylinder of aggregate gland dope surrounding a pair of supporting flagelliform fibers. Low molecular weight organic compounds and salts in this aggregate material confer hygroscopicity (Townley and Tillinghast, 2013), causing it to attract atmospheric moisture, enlarge and then form droplets (Edmonds and Vollrath, 1992). Within each droplet, a glycoprotein core condenses (Fig. 1B). Over the course of a day, the volumes of these hygroscopic droplets change as they respond to changes in environmental humidity (Townley et al., 1991; Opell et al., 2013). Although the allocation of absorbed atmospheric water has not been fully studied, some of it solvates the glycoprotein, ensuring its interaction with a surface, some of it hydrates the glycoprotein core, reducing its viscosity, and some of it probably increases flagelliform fiber extensibility (Sahni et al., 2011, 2014; Opell et al., 2011, 2013; Amarpuri et al., 2015).

Optimal glycoprotein viscosity is crucial for droplet adhesion (Amarpuri et al., 2015). To resist adhesive failure, glycoprotein must be pliable enough to establish contact with an insect surface

¹Department of Biological Sciences, Virginia Tech, Blacksburg, VA 24061, USA.

²Department of Animal and Poultry Sciences, Virginia Tech, Blacksburg, VA 24061, USA.

*Author for correspondence (bopell@vt.edu)

 B.D.O., 0000-0002-1830-0752

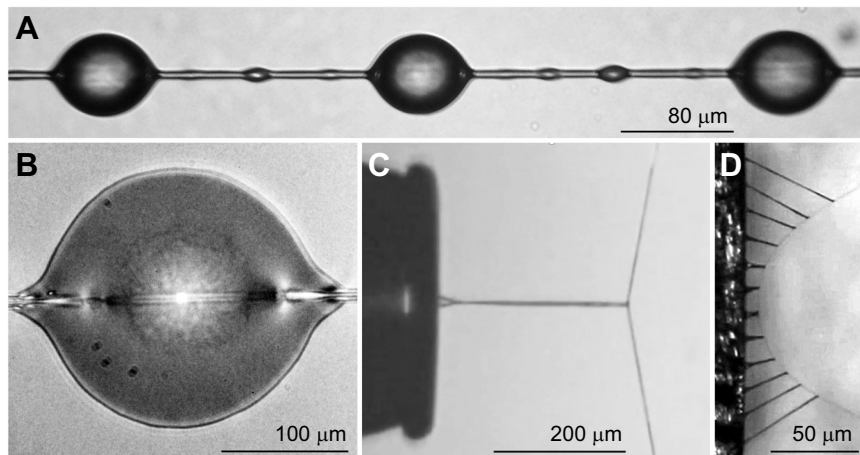


Fig. 1. Viscous threads and droplets. (A–C) *Araneus marmoreus* suspended thread droplets (A), flattened droplet showing glycoprotein core (B) and extended droplet (C). (D) *Neoscona crucifera* thread strand being pulled from a surface, showing successive extension of droplets that contributes to the summation of adhesion.

(Fig. 1B). But the glycoprotein must also be stiff enough to resist cohesive failure when it extends as an insect struggles to escape from a web (Fig. 1C; Amarpuri et al., 2015). When glycoprotein absorbs too much water, it becomes over lubricated and its extensibility is reduced (Sahni et al., 2011; Opell et al., 2013). Moreover, droplet extensibility, in conjunction with flagelliform fiber extensibility, is also responsible for recruiting and summing the adhesion of multiple droplets (Fig. 1D; Opell and Hendricks, 2009), and for absorbing the energy of prey struggle (Sahni et al., 2011). Droplet hygroscopicity and thus glycoprotein viscosity appears to have been tuned to the humidity regime typical of a species' habitat by selection on the salts and low molecular weight organic materials in the droplet's aqueous layer (Townley and Tillinghast, 2013; Amarpuri et al., 2015). When the droplets of species that occupy different habitats were examined, not only did they perform optimally at the humidity typical of each species' habitat but also at these optimal humidities their glycoprotein viscosities were remarkably similar (Amarpuri et al., 2015).

This study tested the hypothesis that humidity-mediated differences in viscous droplet performance translate into differences in insect retention times. We studied threads of the orb weaver *Araneus marmoreus* Clerck 1757, a diurnal species that constructs vertically oriented orb webs in vegetation on forest edges, where humidity remains elevated during the day, and monitors its web using a signal line that extends from the web to the protective confines of the spider's folded leaf retreat (Bradley, 2013; Fasola and Mogavero, 1995; Jennings and Graham, 2007). We inferred the optimal humidity for the adhesive performance of this species' threads from: (1) the conditions of habitats where this species is found, (2) measurements of individual viscous droplet glycoprotein surface area and extensibility, and (3) a model that used these droplet values to estimate the work required to initiate the pull-off of a 4 mm-long capture thread span from a surface. We then tested this prediction by comparing the active struggle time required of house flies to escape from capture threads under different humidities.

Assessing prey retention, particularly in vertical orb webs, is challenging, as it is affected by many factors. These include: (1) the mass of an insect and its impact velocity, (2) the number of capture threads that it strikes, (3) the region of the web a prey strikes, and (4) whether, after struggling free from these threads, the insect tumbles into other capture threads (Blackledge and Zevenbergen, 2006; Zschokke and Nakata, 2015). Moreover, insects often exhibit bouts of escape behavior with intervals of inactivity. To control these variables, we assayed escape behavior by placing an anesthetized house fly wings-downward on three, equally spaced, horizontally

oriented capture thread strands (Fig. 2) and capturing a video of the fly's escape behavior, permitting us to determine the total active struggle time required to overcome thread adhesion.

MATERIALS AND METHODS

Characterizing habitat

We placed a Hobo U23 temperature/relative humidity (RH) data logger (Onset Computer Corporation, Bourne, MA, USA) in each of two habitats where we have observed *A. marmoreus* over the past 12 years. The probe of one logger extended from vegetation of a southeast-facing forest edge at a height of 1.5 m and the probe of the other logger extended from vegetation at the edge of a north-facing forest edge at a height of 1 m. Each logger recorded humidity and temperature at 12 min intervals from 15 August to 15 October, 2016. This interval extended from the time during which *A. marmoreus* are in the last one or two juvenile stadia to the time that most adult females were killed by frosts or died of other causes.

Collecting threads

To ensure that spiders were well nourished and their webs constructed under natural conditions, we collected sectors from orb webs constructed by *A. marmoreus* adult females from their

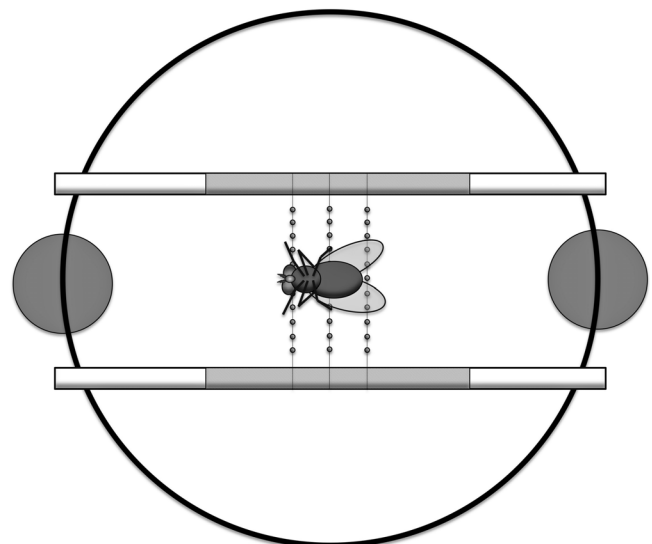


Fig. 2. House fly placement on three capture threads suspended between two supporting bars.

natural habitat on vegetation at the edge of forests near Blacksburg, Montgomery County, VA, USA, between 06:00 h and 08:30 h during September and October. Flagging tape marked the position of each sampled web to prevent resampling. The 13 samples used to characterize droplets were collected during 2013 and 2014 and all still and video images used to describe their properties were completed by 16:00 h on the day of collection. The 14 samples used to evaluate prey retention were collected in 2015 and all videos of insect escape were made by 11:00 h on the day of collection.

Web sectors were collected on 18 cm diameter aluminium rings with a bar across the center. Double-sided 3M tape (no. 9086K29550360, 3M, Maplewood, MN, USA) applied to the 0.6 cm width of the ring and center bar secured the threads without altering the original structure and tension of the web's threads. Immediately after collecting a web sample, this ring was placed in a closed plastic container to prevent contamination by dust and debris. After transporting the webs to the laboratory, we placed 4.0 mm brass bars covered in double-sided carbon tape (cat no. 77816, Electron Microscope Sciences, Hatfield, PA, USA) along the sample's radial threads and across the ring's rim and center bars, enabling us to collect single capture thread strands without compromising their native tensions.

Characterizing thread droplets

Capture thread samples were removed from rings on the carbon tape-covered tips of forceps that were blocked open to accommodate the supports on microscope slide thread samplers and burned free of the web sample using a hot wire probe. These thread samplers consisted of five U-shaped brass struts epoxied at 4.8 mm intervals to microscope slides with their free ends extending upward and covered with double-sided carbon tape (fig. 3 in Opell et al., 2011). Two sets of thread samples were prepared from each web, one to measure glycoprotein contact surface area and one to measure droplet extension. Each set of measurements was made within a temperature- and humidity-controlled chamber that rested on the mechanical stage of a Mitutoyo FS60 inspection microscope (Mitutoyo America Corp., Aurora, IL, USA), where a temperature of 24°C and RHs of 20%, 37%, 55%, 72% and 90% were established (Opell et al., 2013). These values correspond to absolute humidity values of 4.35, 8.05, 11.97, 15.67 and 19.58 g m⁻³, respectively.

Glycoprotein contact area was determined by photographing three suspended droplets (Fig. 1A), recording their sequential positions, flattening these droplets to reveal their spread-out glycoprotein cores (Fig. 1B) by dropping a glass coverslip onto them from a release mechanism contained within the observation chamber, and, finally, rephotographing each of these droplets (Opell et al., 2013). We used ImageJ (Rasband 1997–2012) to measure the length (DL; dimension parallel to the axial fiber) and width (DW) of suspended droplets and the surface areas of flattened droplets and their glycoprotein cores. We determined droplet volume (DV) using the following formula (Opell and Schwend, 2007; Liao et al., 2015):

$$DV = (2\pi \times DW^2 \times DL)/15. \quad (1)$$

The volume of a glycoprotein core was computed at each RH by first dividing a droplet's volume by its flattened area to determine the mean thickness of the flattened droplet. This thickness was then multiplied by the surface area of the flattened droplet's core to determine glycoprotein volume. For each droplet, the ratio of glycoprotein volume to droplet volume was determined. The mean of these values was calculated for each individual. An individual

spider's humidity-specific glycoprotein ratio was then multiplied by the volume of the individual's droplet that was to be extended to infer the volume of glycoprotein within this droplet.

In preparing suspended droplets for extension measurements, we ensured that the probe used to contact and extend a droplet contacted only a single droplet. We did so by using a minuten insect pin moistened with distilled water to move away droplets that were adjacent to the test droplet located at the center of the thread strand. This process retained the aqueous coating of the strand's axial fibers, as demonstrated by the formation of small droplets similar to those often present between the large primary droplets of many viscous threads (Fig. 1A). Prior to each extension, we photographed the isolated suspended droplet and used this image to infer its glycoprotein volume as described above. A steel probe, cleaned with 100% ethanol on a Kimwipe® before each use, was then inserted through a port in the side of the test chamber and its 413 µm-wide polished tip aligned and brought into contact with the focal droplet. To ensure full droplet adhesion, the probe was pressed against the droplet until it was deflected by a distance of 500 µm. A 60 frames s⁻¹ video then recorded the droplet's extension as the thread was withdrawn from the probe at a velocity of 69.6 µm s⁻¹ by a stepping motor, which moved the mechanical stage on which the observation chamber rested. From these videos, we measured the length of the extending droplet filament just before its release from the probe.

To determine the change in water volume within a viscous droplet, we subtracted the mean droplet volume at 20% RH from that at each of the other RHs. We determined the change in water volume within a droplet's glycoprotein core by subtracting the mean glycoprotein volume at 20% RH from that at each of the other RHs. We then determined the change in water content of the aqueous layer at each of the four higher RHs by subtracting the change in water content of the droplet's glycoprotein core from the total change in droplet water content.

Modeling work required to initiate thread pull-off

When force is applied to a viscous thread that has adhered to a surface, the droplets extend (Fig. 1D) until the outermost one pulls from a surface and inner droplets successively extend and release. The thread's configuration just prior to the initiation of pull-off, as marked by the release of the outermost droplet, represents the point at which maximum thread adhesion is achieved (Opell and Hendricks, 2009). The work required to extend the droplet to this point is directly related to the volume of droplet's glycoprotein (V), the stiffness of its glycoprotein (S) and the distance over which the glycoprotein (droplet) is extended (D). Volume and extension increase, up to a point, as humidity increases, whereas stiffness decreases.

Araneus marmoreus viscous threads have an average of 3.7 droplets per mm (Opell and Hendricks, 2009), or 15 droplets per 4 mm span. Because the viscous thread's axial lines are very extensible, the two outermost droplets have extended much further than the inner droplets by the time the outer droplets release (Fig. 1D). Our simple model assumes that the thread's paired support lines take the shape of a parabola, as suggested by our current studies (B.D.O., unpublished observations). Thus, as humidity increases, the total extension of the droplets in a span will increase because the stiffness of their glycoprotein decreases (Fig. 3A,B, 20–72% RH). This continues until droplet extension diminishes as the glycoprotein within a droplet begins to experience adhesive failure at its contact footprint and cohesive failure in its extending filament (Fig. 3A, 90% RH).

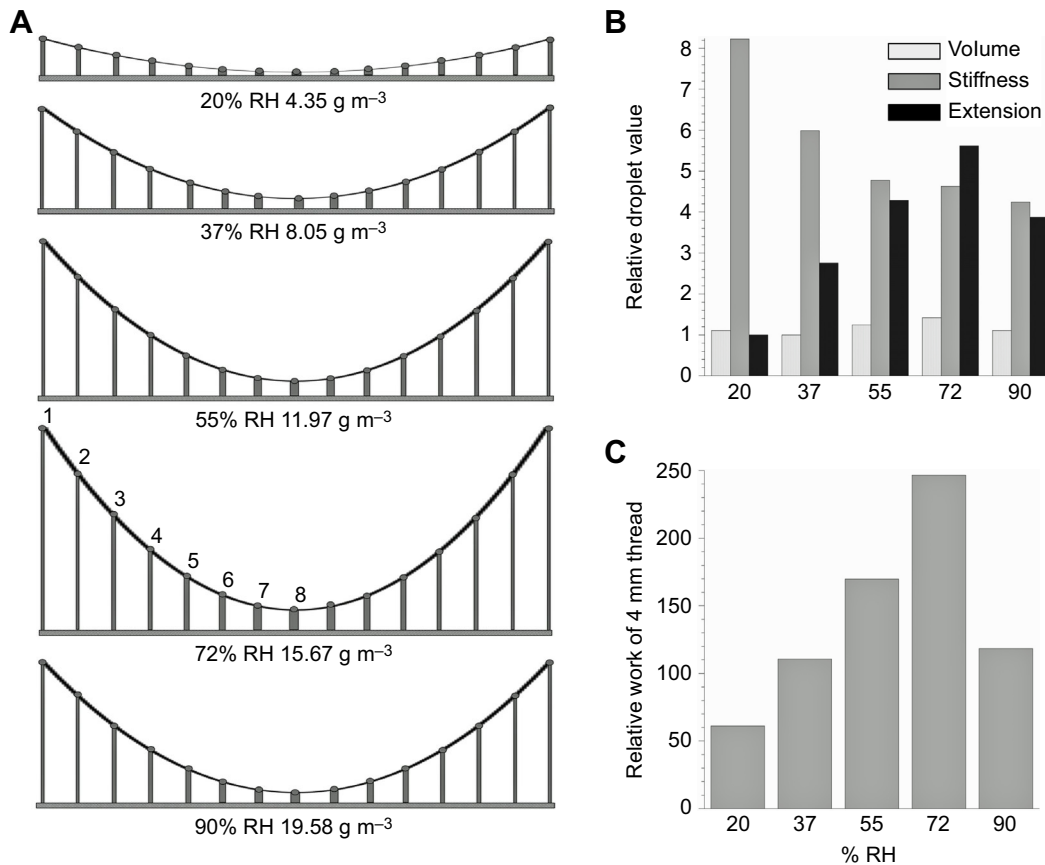


Fig. 3. Procedures used to model the relative work of extending the 15 droplets in a 4 mm span of *A. marmoreus* viscous thread to the point of pull-off. (A) Configurations of the thread extension at each of the five experimental relative humidities (RHs), as established from parabolas, with their terminal points (droplet 1) set to maximum droplet extension and their midpoints (droplet 8) set to 10% of this value. (B) The relative volume, stiffness and extension of droplets at each RH. (C) The resulting relative work required to extend a thread span to the point of pull-off at each RH.

Based on this simple model, we computed the work (W) required to initiate the pull-off of a 4 mm span of thread as:

$$W = \sum(V \times S \times D).$$

In this model, we used relative values, determined by assigning the smallest value of each index a value of 1 (Table 1). These indices were derived from the measurements described in the previous section, as reported in Table 2, and include glycoprotein volume, glycoprotein stiffness (glycoprotein volume/glycoprotein surface area, a value equal to the thickness of the flattened glycoprotein core), and the expressed extension of each of the span's 15 droplets. The two outer droplets (labeled 1 in Fig. 3A) were assigned the maximum droplet extension value and the innermost droplet (droplet 8 in Fig. 3A) a value that was 10% of this. We then fitted a parabola to these three points (Fig. 3A) and measured the lengths of droplets 2–7.

Positioning threads for retention study

We used tweezers with tips that were blocked open to a width of 2 cm and wrapped in carbon tape to collect a single span of capture thread from the web sample. Three 18 mm thread strands were placed 2.3 mm apart on parallel bars covered in 3M tape (no. 9086K29550360, 3M) (Fig. 2). The bars were glued to a 50 mm ring from which two mounting rods extended, allowing us to position this sample holder horizontally during observations of insect retention.

We assayed insect retention using adult *Musca domestica* house flies (item 100002365, Evergreen Growers Supply, Oregon City, OR, USA) reared from pupae. A sample of six flies had a mean mass of 12.01 ± 0.88 mg, a head width of 222 ± 4 μ m, a notum width of 211 ± 7 μ m and an individual wing width of 247 ± 11 μ m. Each fly was anesthetized with CO_2 gas for 3–4 s and was then placed wings-downward on the three capture threads with its head touching the first thread and the wings touching the second and third threads (Fig. 2).

Establishing RH for retention studies

Target RHs of 37%, 55% and 72% were established in three $30.5 \times 49.5 \times 31.8$ cm Plexiglas desiccator chambers. The 37% RH chamber was equipped with a small Ivation Peltier dehumidifier (model 236072) and a tray of silica gel desiccant. Two ice packs were placed in the chamber to offset the dehumidifier's thermal input. As laboratory humidity was slightly below 55%, we regulated the humidity of the 55% RH chamber by gently exhaling into the chamber. A small Foxwill Volcano Ultrasonic Humidifier 160 ml USB mini humidifier and circulating fan established 72% RH. We monitored humidity with a Fisher digital hygrometer (model 11-661-7A) and temperature with a Fisher digital thermometer (model 11-661-8), recording the values under which each test was conducted.

Assessing fly retention

We placed a thread sample holder into a humidity chamber before anesthetizing a fly, allowing capture threads to acclimate to the test humidity for 1–2 min and then placed a fly, wings downward, on the

Table 1. Values used in computations of the work required for thread extension to the initiation of pull-off

Droplet feature	% RH				
	20	37	55	72	90
Relative glycoprotein volume	1.11	1.00	1.25	1.42	1.11
Glycoprotein stiffness	8.23	5.99	4.78	4.63	4.25
Relative max. extension	1.00	2.76	4.29	5.62	3.88
Length droplet 1	1.00	2.76	4.29	5.62	3.88
Length droplet 2	0.78	2.15	3.32	4.34	2.95
Length droplet 3	0.58	1.57	2.40	3.15	2.12
Length droplet 4	0.39	1.10	1.68	2.21	1.45
Length droplet 5	0.26	0.75	1.12	1.49	0.96
Length droplet 6	0.17	0.46	0.71	0.98	0.58
Length droplet 7	0.11	0.31	0.47	0.68	0.42
Length droplet 8	0.10	0.28	0.43	0.56	0.39
Relative work droplet 1	9.14	16.53	25.63	36.95	18.30
Relative work droplet 2	7.13	12.88	19.84	28.53	13.92
Relative work droplet 3	5.30	9.40	14.34	20.71	10.00
Relative work droplet 4	3.56	6.59	10.04	14.53	6.84
Relative work droplet 5	2.38	4.49	6.69	9.80	4.53
Relative work droplet 6	1.55	2.76	4.24	6.44	2.74
Relative work droplet 7	1.00	1.86	2.81	4.47	1.98
Relative work droplet 8	1.00	1.68	2.57	3.68	1.84
Total relative work	61.12	110.70	169.75	246.55	118.46

Glycoprotein stiffness was calculated as volume/area. Relative glycoprotein volume and maximum extension values are derived from values given in Table 2. Other relative extension values are derived from thread configurations shown in Fig. 3A.

threads. After the anesthetized fly was placed on threads, we filmed its behavior at 60 frames s^{-1} with a Canon Vixia HF 610, HD camcorder (Movie 1). Using iMovie, we analyzed each video to determine the length of time a fly was actively struggling to leave the web. We characterized active struggle as rapid wing flapping, which was sometimes also associated with rapid leg movements. We recorded both the number of these active bouts and their duration, summing them to determine a fly's total struggle time.

Statistical analysis

We used JMP (SAS Institute, Cary, NC, USA) to analyze data and considered comparisons with $P \leq 0.05$ as significant. All tests are two-tailed. The normal distribution of values was assessed with a Shapiro–Wilk W -test, with values of $P > 0.05$ being considered normal.

Table 2. Characteristics of droplets used to evaluate the effect of RH on performance

Droplet feature	%RH				
	20	37	55	72	90
Glycoprotein area and vol. sample size	13	13	13	13	12
Length (μm)	68 \pm 3.2	68 \pm 3.8	66 \pm 3.2	73 \pm 3.3	76 \pm 3.3
Width (μm)	53 \pm 2.7	53 \pm 3.4	51 \pm 3.0	58 \pm 3.1	60 \pm 3.0
Volume (μm^3)	87,258 \pm 11,681	92,548 \pm 16,268	81,329 \pm 12,601	114,757 \pm 16,270	124,531 \pm 18,046
Glycoprotein area (μm^2)	3349 \pm 581	4127 \pm 1003	6476 \pm 2062	7573 \pm 2688	6481 \pm 2572
Glycoprotein vol. (μm^3)	27,548 \pm 5736	24,709 \pm 7620	30,942 \pm 11,059	35,056 \pm 13,450	27,528 \pm 10,559
GV/DV ratio	0.31 \pm 0.039	0.25 \pm 0.047	0.28 \pm 0.070	0.23 \pm 0.064	0.19 \pm 0.043
Glycoprotein area/vol.	0.132 \pm 0.0096	0.200 \pm 0.0149	0.258 \pm 0.0250	0.259 \pm 0.0243	0.228 \pm 0.0111
Extended droplet sample size	13	13	13	13	12
Length (μm)	64 \pm 2.4	69 \pm 2.6	70 \pm 3.1	72 \pm 3.4	77 \pm 3.8
Width (μm)	49 \pm 2.0	54 \pm 2.3	55 \pm 2.6	57 \pm 2.9	61 \pm 3.4
Volume (μm^3)	68,790 \pm 7541	91,310 \pm 10,699	96,961 \pm 12,100	108,270 \pm 15,872	129,193 \pm 20,152
Inferred glycoprotein vol. (μm^3)	20,190 \pm 3107	22,326 \pm 5050	34,375 \pm 11,907	35,373 \pm 14,031	26,653 \pm 8545
Droplet extension (μm)	755 \pm 98	2081 \pm 252	3239 \pm 391	4244 \pm 767	2928 \pm 676

GV, glycoprotein volume; DV, droplet volume. Data are means \pm 1 s.e.m.

RESULTS

Habitat humidity

At the two representative *A. marmoreus* sites, RH decreased to 67–76% and temperature increased to 23–24°C by mid-afternoon, resulting in absolute humidity remaining between 14.5 and 15.8 g m^{-3} (Fig. 4), values that most closely match the 15.73 g m^{-3} mean value of our 72% RH treatment (Table 3).

Viscous droplet and performance

Table 2 summarizes the effect of humidity on droplet features and performance. Mean droplet dimension (average of droplet length and width) increased slightly in the two highest RHs, although the ratio of droplet length (direction parallel to droplet axial lines) to width changed little as humidity increased (Fig. 5). Despite this, there was a precipitous drop in free absorbed water present in a droplet's aqueous material at 55% RH followed by increases at 72% and 90% RH. The volume of water absorbed by a droplet's glycoprotein core increased at 55% and 72% RH and decreased at 90% RH.

To reduce the effect of inter-individual droplet size, we plotted both glycoprotein contact area and droplet extension values relative to the glycoprotein volume of an individual's droplet. The greatest relative glycoprotein contact area occurred at 55% and 72% RH, with relative droplet extension peaking at 72% (Fig. 6), causing us to hypothesize that capture threads should retain house flies to the greatest length of time at 72% RH.

The model of relative changes in glycoprotein features (Table 1, Fig. 3B) showed that relative glycoprotein volume increased slightly as humidity increased to 72% and then decreased, whereas relative glycoprotein stiffness decreased greatly as humidity increased. Relative droplet extension increased continually to 72% and then decreased. When these values were used to approximate the relative work of adhesion necessary to extend a 15 droplet, 4 mm span of capture thread to the point of pull-off, they resulted in steadily increasing work up to 72% RH and a marked decrease in work at 90% RH (Fig. 3C). Thus, these results support those of single droplet performance described in the previous paragraph in predicting that *A. marmoreus* capture threads should perform optimally at 72% RH.

Insect retention

Table 3 summarizes insect retention results and Table S1 provides the core results. We controlled RH within narrow limits, but mean

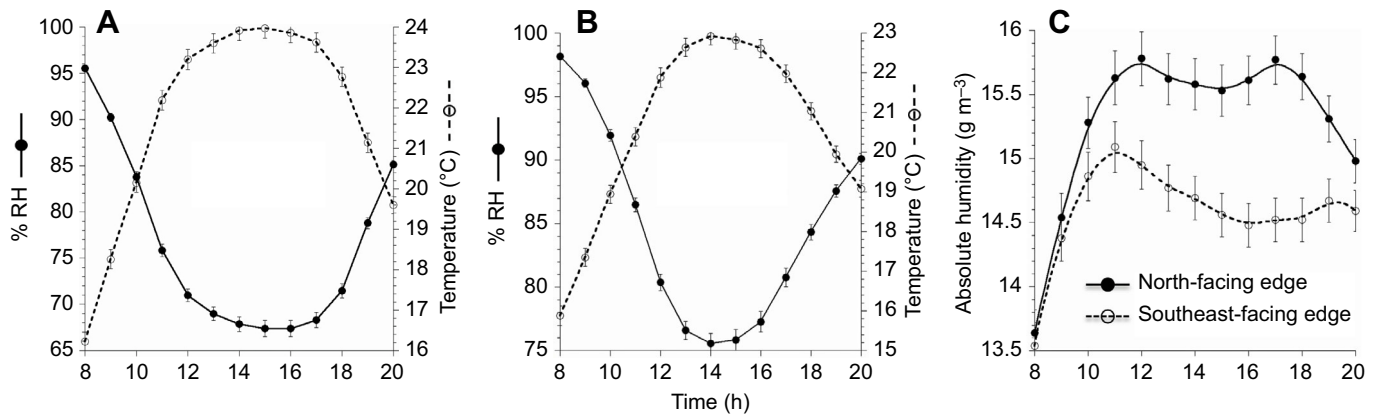


Fig. 4. Mean RH, temperature and absolute humidity recorded at two forest edge sites where *A. marmoreus* have been observed. (A) Southeast-facing edge. (B) North-facing edge. (C) Absolute humidity data for southeast- and north-facing edge. Error bars are ± 1 s.e.m.

temperature differed among treatments, being 1.2°C higher at 37% RH and 1.4°C lower at 72% RH than at 55% RH. However, regressions showed no relationship between temperature and total struggle time for 37%, 55% and 72% RH treatments ($P=0.2779$, 0.7174 , 0.1322 , $R^2=0.097$, 0.011 , 0.179 , respectively). There were no inter-humidity differences among the slopes of these regression lines ($P=0.1638$). Neither total in-web time nor the number of active struggle bouts differed among RHs (Table 3). Although a Wilcoxon test showed no overall difference in fly struggle time among RHs (Table 3), the struggle time at 72% RH was twice that at 37% and 55% RH and a Wilcoxon each-pair test identified a difference between 37% and 72% RH values ($P=0.0386$).

Mean individual struggle time ranged from 3.33 to 34.67 s and averaged 14.26 ± 2.98 s (mean \pm s.e.m.). We attributed some of this variance to inter-spider differences in capture thread adhesion. We addressed this by first averaging the active struggle times required

for flies to escape from an individual spider's threads at 37%, 55% and 72% RH. We then subtracted this mean value from the active struggle time required to escape from this individual's threads at each experimental humidity to compute an index we term fly struggle time difference (FSTD).

A linear regression showed no experiment-wide effect of temperature on FSTD ($P=0.3259$, $R^2=0.024$), with quadratic and exponential 3P models showing little improvement ($R^2=0.031$ and 0.030 , respectively). A linear regression of FSTD on measured RH and temperature was marginally insignificant ($P=0.0503$), with RH but not temperature contributing to this model ($P=0.0259$ and 0.5068 , respectively). Measured RH was significantly and positively related to FSTD ($P=0.0179$). We also determined the difference between each individual's mean experimental temperature (which ranged from 23.17 to 27.07°C) and the temperature at which each of its humidity trials were conducted, an index we term temperature difference (TD). Regressions showed no relationship between TD and FSTD across the data set or for 37%, 55% and 72% RH treatments ($P=0.1806$, 0.6131 , 0.1093 and 0.4843 , respectively). A regression of FSTD on measured RH and

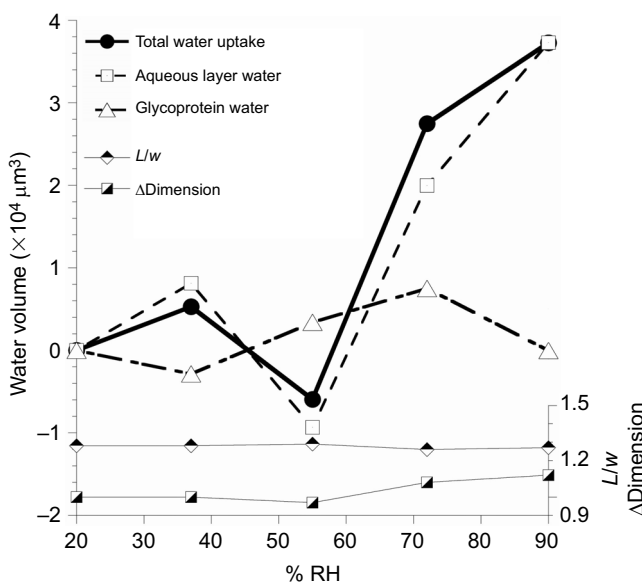


Fig. 5. Changes in the volume and distribution of water within a viscous droplet with changes in RH. Values were determined from data presented in Table 2. The two lower lines describe the length/width (L/w) ratio of droplets at each humidity and the proportional change (Δ) in mean droplet dimension from that at 20% RH. The three upper lines describe changes in total water droplet from values at 20% RH and the allocation between the droplet's aqueous layer and glycoprotein core.

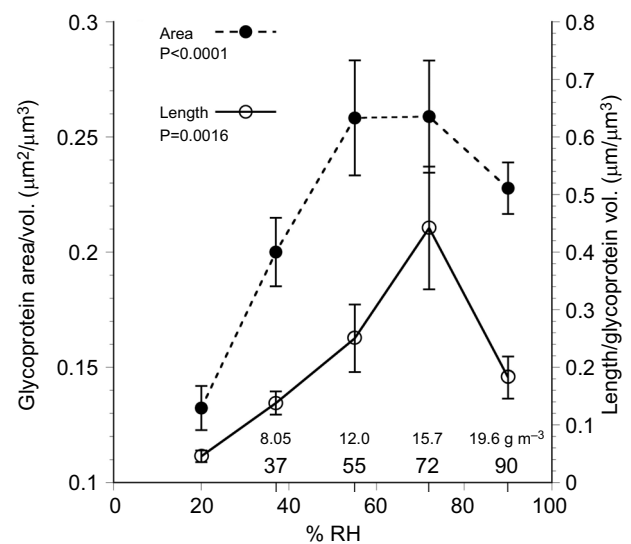


Fig. 6. Comparison of glycoprotein contact area per glycoprotein volume and maximum droplet extension per glycoprotein volume. Sample size: 20–72% RH, $n=13$; 90% RH, $n=12$. Data are means ± 1 s.e.m.; P -values for Wilcoxon tests are shown.

Table 3. Experimental temperature and humidity, and in-web time, number of struggle bouts and total struggle time of flies

% RH	Temperature (°C)	Absolute humidity (g m ⁻³)	In-web time (s)	Struggle bouts	Struggle time (s)
37.9±0.6	26.4±0.4*	9.47±0.24*	123.3±27.8	4.3±1.3	10.40±4.60
54.9±0.3*	25.2±0.4*	12.80±0.24*	62.4±13.7	3.3±0.5	10.79±2.23
72.9±0.3*	23.8±0.2	15.73±0.23*	119.1±29.1	5.9±1.4	21.59±5.41
<i>P</i> -value	W 0.0003	A 0.0001	W 0.1188	W 0.3063	W 0.0846

Sample size, $n=14$. Data are means±1 s.e.m. *Values that were normally distributed, as identified by a Shapiro–Wilk W -test $P>0.05$. P -values for comparisons are for Wilcoxon (W) or ANOVA (A) tests.

TD was significant ($P=0.0317$), with RH but not TD contributing to this model ($P=0.0244$ and 0.2454 , respectively). Therefore, we assume that temperature can be eliminated as a contributing variable in subsequent analyses of the effect of humidity on FSTD.

Shapiro–Wilk tests showed that FSTD was normally distributed at 55% and 72% RH, but not at 37% RH ($P=0.7732$, 0.0814 and 0.0170 , respectively), requiring the use of non-parametric statistics. A Wilcoxon test showed that RH affected FSTD ($P=0.0187$), with Wilcoxon each-pair tests identifying differences between values at 37% and 72% RH ($P=0.0082$) and between those at 55% and 72% RH ($P=0.0326$), but not between those at 37% and 55% RH ($P=0.8362$) (Fig. 7).

DISCUSSION

Environmental humidity plays a critical role in the function of an orb web from the time that it is constructed until the time that it is taken down. High humidity during web construction facilitates the self-assembly of viscous capture threads. Changes in humidity over the course of a day affect the web's ability to both withstand prey impact and retain intercepted prey. Webs of *Argiope trifasciata* and *Nephila clavipes* were better able to absorb the kinetic energy of simulated prey strikes at high humidity than at low humidity (Boutry and Blackledge, 2013). Our study demonstrates that fine-scale, humidity-mediated changes in capture thread droplet adhesion affect prey retention times. Finally, when a web is taken down and its silk ingested during the high humidity of the evening or early morning, the fully hydrated viscous droplets supply a spider with both recyclable protein and water (Townley and Tillinghast, 1988; Edmonds and Vollrath, 1992).

Our observations support the hypothesis that humidity-mediated changes in *A. marmoreus* viscous thread droplets and threads, as

assessed by laboratory tests, translate into measurable differences in the retention time of actively struggling house flies. House flies were retained an average of 11 s longer at 72% RH than at 37% and 55% RH. This difference in prey retention is ecologically significant, as the short time after an insect strikes a web and before a spider commences wrapping the insect is the insect's only opportunity to escape from the web. A study of the retention of hanging flies, and small and large grasshoppers by orb webs from which spiders were removed showed that of the insects that escaped from webs within a 180 s trial period, 18% did so within 1 s of striking the web (Blackledge and Zevenbergen, 2006). Our study used prey retention time to evaluate the performance of capture threads. However, retention time should be directly related to the size of prey that a web can retain. For large orb weavers like *A. marmoreus*, these large prey are crucial because they comprise the greatest proportion of a spider's total food intake (Venner and Casas, 2005), although aspects of this large profitable prey hypothesis have been called into question (Eberhard, 2013). Thus, the hygroscopicity of viscous threads has probably been tuned to the humidity of a species' habitat by selection favoring an increase in both the number and size of prey that a web captures in ways that facilitate not only spider survival but also the total number of eggs produced.

The performance of *A. marmoreus* threads is consistent with this species' occupation of forest edge habitats (Bradley, 2013; Fasola and Mogavero, 1995; Jennings and Graham, 2007), where humidity remains elevated during the late morning and early afternoon hours (Fig. 4). While recordings from only two sites do not fully characterize this species' habitat, they combine with analyses of droplet and thread performance to suggest that *A. marmoreus* viscous threads have been selected to function in moderately high humidities. Moreover, in the two sampled habitats, absolute humidity changed little from mid-morning to late afternoon, indicating that these threads encounter more stable conditions than suggested by RH alone.

Humidity affects viscous droplets and threads in many ways. As humidity increases, more water is absorbed by a droplet's glycoprotein, reducing its viscosity and causing it to have a greater surface area of contact and extend further before releasing until, at the highest humidity, the glycoprotein becomes over-lubricated (Sahni et al., 2011; Opell et al., 2013) and extension decreases (Fig. 6). However, the effect of humidity on water allocation within a droplet appears more complicated, as reflected by a large drop in the free water content of the droplet's aqueous material at 55% RH (Fig. 5). A similar deflection in droplet volume at 55% RH was observed in *Argiope aurantia* (see fig. 9A of Opell et al., 2013). The formula used to compute droplet volume is unaffected by changes in droplet volume at different humidities (Liao et al., 2015) and the drop in free water within the aqueous layer at 55% RH seems too great to be explained by small inaccuracies in our method of assessing the change in glycoprotein water content, particularly as glycoprotein volume is only 20–30% of droplet volume (Table 1, GV/DV ratio). This dip in water content is consistent with a study of *Araneus diadematus* orb webs, which

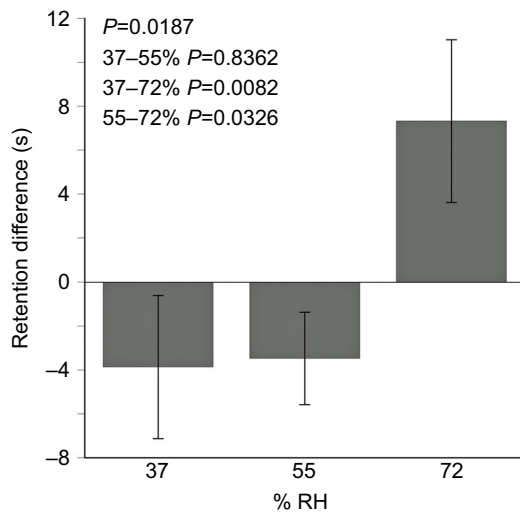


Fig. 7. Comparison of the deviation of house fly retention time from the mean retention time of an individual spider's threads. $n=14$. Data are means±1 s.e.m.; P -values for Wilcoxon overall and each-pair tests are shown.

showed that at about 48% RH, whole-web samples, water-soluble and -insoluble, and ethanol-soluble and -insoluble fractions of webs exhibited a dip in weight gain as humidity increased (see fig. 2 of Vollrath et al., 1990). That study also showed that the *N*-acetyltaurine, GABamide, and sodium isethionate found in these viscous threads did not begin to absorb atmospheric moisture until RH increased to 42–46%. Thus, it appears that two overlapping phenomena may underlie the apparent dip in the aqueous layer's water volume at 55% RH: (1) more water is taken up by the flagelliform fibers that pass through the droplet and by the low molecular weight compounds within the aqueous layer when humidity exceeds 40% and (2) less-hygroscopic compounds, like those mentioned above, begin to add water to the droplet when humidity exceeds 55%. It may be possible to distinguish these two events by measuring droplet and glycoprotein volumes at smaller intervals within the 40–60% RH range.

Our simple model of the work required to extend a thread span to the initiation of pull-off shows how humidity-mediated changes in glycoprotein volume and viscosity impact the thread span's ability to resist an insect's struggle (Fig. 3). Our model showed that changes in glycoprotein volume have the least effect and changes in glycoprotein extensibility the greatest effect on thread performance. As humidity increases and the glycoprotein becomes less viscous, less energy is required for its extension. Thus, in the context of a thread span, greater droplet extensibility allows more droplets to extend a greater distance, resulting in more energy being absorbed by the thread span. However, actual thread performance begins to deviate from this model at very high humidity, because some droplets slide and merge or their extending filaments combine to form a sheet, leading to configurations that are more challenging to model (Amarpuri et al., 2015; B.D.O., unpublished observations).

Acknowledgements

Sheree Andrews provided technical support and helpful comments on the manuscript. Sarah Stellwagen captured some of the images and videos used in droplet analyses. Sarah Helweg measured the lengths and widths of droplets. Robin Andrews discussed and provided perspective on the statistical analyses.

Competing interests

The authors declare no competing or financial interests.

Author contributions

B.D.O. designed the study, constructed instruments and chambers, collected web samples, supervised observations and preliminary statistical analyses, conducted final statistical analyses and modeling, and prepared the final manuscripts and Figs 1 and 3–5. K.E.B., M.K.G. and M.X.R. prepared thread samples, regulated the temperature and humidity in observation chambers, captured and analyzed insect escape videos, entered data, performed preliminary statistical analyses, and helped prepare the first manuscript draft. K.E.B. prepared Fig. 2. M.L.H. measured the surface areas of flattened droplets and the extensions of suspended droplets, computed glycoprotein volumes and assisted in droplet performance analysis.

Funding

National Science Foundation grant IOS-1257719 supported this study.

Supplementary information

Supplementary information available online at <http://jeb.biologists.org/lookup/doi/10.1242/jeb.148080.supplemental>

References

- Agnarsson, I., Boutry, C., Wong, S.-C., Baji, A., Dhinojwala, A., Sensenig, A. T. and Blackledge, T. A. (2009). Supercontraction forces in spider dragline silk depend on hydration rate. *Zoology* **112**, 325–331.
- Amarpuri, G., Zhang, C., Diaz, C., Opell, B. D., Blackledge, T. A. and Dhinojwala, A. (2015). Spiders tune glue viscosity to maximize adhesion. *ACS Nano* **9**, 11472–11478.
- Blackledge, T. A. and Zevenbergen, J. M. (2006). Mesh width influences prey retention in spider orb webs. *Ethology* **112**, 1194–1201.
- Blamires, S. J. (2010). Plasticity in extended phenotypes: orb web architectural responses to variations in prey parameters. *J. Exp. Biol.* **213**, 3207–3212.
- Blamires, S. J., Tseng, Y.-H., Wu, C.-L., Toft, S., Raubenheimer, D. and Tso, I.-M. (2016). Spider web and silk performance landscapes across nutrient space. *Sci. Rep.* **6**, 26383.
- Boutry, C. and Blackledge, T. A. (2013). Wet webs work better: humidity, supercontraction and the performance of spider orb webs. *J. Exp. Biol.* **216**, 3606–3610.
- Boutry, C. and Blamires, S. J. (2013). Plasticity in spider webs and silk: an overview of current evidence. In *Spiders: Morphology, Behavior and Geographic Distribution* (ed. M. Santerre), pp. 1–46. New York: Nova.
- Bradley, R. A. (2013). *Common Spiders of North America*. Berkeley, CA: University of California Press.
- Chacón, P. and Eberhard, W. G. (1980). Factors affecting numbers and kinds of prey caught in artificial spider webs with considerations of how orb-webs trap prey. *Bull. Br. Arach. Soc.* **5**, 29–38.
- Dawkins, R. (1982). *The Extended Phenotype: The Long Reach of the Gene*. Oxford: Oxford University Press.
- Eberhard, W. G. (1989). Effects of orb-web orientation and spider size on prey retention. *Bull. Br. Arach. Soc.* **8**, 45–48.
- Eberhard, W. G. (2013). The rare large prey hypothesis for orb web evolution: a critique. *J. Arachnol.* **41**, 76–80.
- Edmonds, D. T. and Vollrath, F. (1992). The contribution of atmospheric water vapour to the formation and efficiency of a spider's web. *Proc. R. Soc. Lond. B Biol. Sci.* **248**, 145–148.
- Fasola, M. and Mogavero, F. (1995). Structure and habitat use in a web-building spider community in northern Italy. *Boll. Di Zool.* **62**, 159–166.
- Herberstein, M. E. and Tso, I. M. (2011). Spider webs: evolution, diversity and plasticity. In *Spider Behaviour: Flexibility and Versatility* (ed. M. E. Herberstein), pp. 57–98. Cambridge: Cambridge University Press.
- Jennings, D. T. and Graham, F. (2007). *Spiders (Arachnida: Araneae) of Milbridge, Washington County, Maine*. Northern Research Station General Technical Report. Newtown Square, PA. https://www.nrs.fs.fed.us/pubs/gtr/gtr_nrs16.pdf
- Liao, C.-P., Blamires, S. J., Hendricks, M. L. and Opell, B. D. (2015). A re-evaluation of the formula to estimate the volume of orb web glue droplets. *J. Arachnol.* **43**, 97–100.
- Opell, B. D. and Hendricks, M. L. (2009). The adhesive delivery system of viscous capture threads spun by orb-weaving spiders. *J. Exp. Biol.* **212**, 3026–3034.
- Opell, B. D. and Schwend, H. S. (2007). The effect of insect surface features on the adhesion of viscous capture threads spun by orb-weaving spiders. *J. Exp. Biol.* **210**, 2352–2360.
- Opell, B. D., Karinshak, S. E. and Sigler, M. A. (2011). Humidity affects the extensibility of an orb-weaving spider's viscous thread droplets. *J. Exp. Biol.* **214**, 2988–2993.
- Opell, B. D., Karinshak, S. E. and Sigler, M. A. (2013). Environmental response and adaptation of glycoprotein glue within the droplets of viscous prey capture threads from araneoid spider orb-webs. *J. Exp. Biol.* **216**, 3023–3034.
- Opell, B. D., Andrews, S. F., Karinshak, S. E. and Sigler, M. A. (2015). The stability of hygroscopic compounds in orb-web spider viscous thread. *J. Arachnol.* **43**, 152–157.
- Sahni, V., Blackledge, T. A. and Dhinojwala, A. (2011). Changes in the adhesive properties of spider aggregate glue during the evolution of cobwebs. *Sci. Rep.* **1**, 41.
- Sahni, V., Dhinojwala, A., Opell, B. D. and Blackledge, T. A. (2013). Prey capture adhesives produced by orb-weaving spiders. In *Biotechnology of Silk. Biologically-Inspired Systems 5* (ed. T. Asakura and T. Miller), pp. 203–217. Dordrecht: Springer.
- Sahni, V., Miyoshi, T., Chen, K., Jain, D., Blamires, S. J., Blackledge, T. A. and Dhinojwala, A. (2014). Direct solvation of glycoproteins by salts in spider silk glues enhances adhesion and helps to explain the evolution of modern spider orb webs. *Biomacromolecules* **15**, 1225–1232.
- Scharf, I., Lubin, Y. and Ovadia, O. (2011). Foraging decisions and behavioural flexibility in trap-building predators: a review. *Biol. Rev.* **86**, 626–639.
- Sensenig, A. T., Lorentz, K. A., Kelly, S. P. and Blackledge, T. A. (2012). Spider orb webs rely on radial threads to absorb prey kinetic energy. *J. R. Soc. Interface* **9**, 1880–1891.
- Stellwagen, S. D., Opell, B. D. and Short, K. G. (2014). Temperature mediates the effect of humidity on the viscoelasticity of glycoprotein glue within the droplets of an orb-weaving spider's prey capture threads. *J. Exp. Biol.* **217**, 1563–1569.
- Stellwagen, S. D., Opell, B. D. and Clouse, M. E. (2015). The impact of UVB radiation on the glycoprotein glue of orb-weaving spider capture thread. *J. Exp. Biol.* **218**, 2675–2684.
- Townley, M. A. and Tillinghast, E. K. (1988). Orb web recycling in *Araneus cavaticus* (Araneae, Araneidae) with an emphasis on the adhesive spiral component, Gabamide. *J. Arachnol.* **16**, 303–319.
- Townley, M. A. and Tillinghast, E. K. (2013). Aggregate silk gland secretions of araneoid spiders. In *Spider Ecophysiology* (ed. W. Nentwig), pp. 283–302. New York: Springer-Verlag.

- Townley, M. A., Bernstein, D. T., Gallanger, K. S. and Tillinghast, E. K.** (1991). Comparative study of orb-web hygroscopicity and adhesive spiral composition in three areneid spiders. *J. Exp. Biol.* **259**, 154–165.
- Townley, M. A., Tillinghast, E. K. and Neefus, C. D.** (2006). Changes in composition of spider orb web sticky droplets with starvation and web removal, and synthesis of sticky droplet compounds. *J. Exp. Biol.* **209**, 1463–1486.
- Tso, I.-M., Chiang, S.-Y. and Blackledge, T. A.** (2007). Does the giant wood spider *Nephila pilipes* respond to prey variation by altering web or silk properties? *Ethology* **113**, 324–333.
- Venner, S. and Casas, J.** (2005). Spider webs designed for rare but life-saving catches. *Proc. R. Soc. B Biol. Sci.* **272**, 1587–1592.
- Vollrath, F., Fairbrother, W. J., Williams, R. J. P., Tillinghast, E. K., Bernstein, D. T., Gallagher, K. S. and Townley, M. A.** (1990). Compounds in the droplets of the orb spider's viscous spiral. *Nature* **345**, 526–528.
- Wu, C.-C., Blamires, S. J., Wu, C.-L. and Tso, I.-M.** (2013). Wind induces variations in spider web geometry and sticky spiral droplet volume. *J. Exp. Biol.* **216**, 3342–3349.
- Zschokke, S. and Nakata, K.** (2015). Vertical asymmetries in orb webs. *Biol. J. Linnean Soc.* **114**, 659–672.